INTERNATIONAL JOURNAL FOR NUMERICAL METHODS IN FLUIDS, VOL. 11, 555–569 (1990)

INFINITE ELEMENTS FOR WATER WAVE RADIATION AND SCATTERING*

H. S. CHEN

NOAA/NWS/NMC, Ocean Products Center, 5200 Auth Road, Washington, DC 20233, U.S.A.

SUMMARY

The infinite element method is employed to approximate the solutions of Webster's horn equation and Berkhoff's equation for water wave radiation and scattering in an unbounded domain. Functionals based on the first variational principle are presented. Two new infinite elements, which exactly satisfy the one- and two-dimensional Sommerfeld radiation condition, are presented; the simple shape functions are constructed on the basis of the asymptotic behaviour of the scattered wave at infinity. All the integrals in the functionals involving each infinite element are integrated analytically and, as a result, no numerical integration is required. The programming requirements and computational efficiency are essentially no different than those of the conventional finite element method. For the test cases presented, the numerical results are acceptably accurate when compared with the existing solutions and laboratory data.

KEY WORDS Infinite element Unbounded domain Radiation condition Wave radiation Scattering

INTRODUCTION

The boundary value problem associated with water wave radiation and scattering of coastal or offshore water is usually formulated in an unbounded domain, because the Sommerfeld radiation condition must be imposed at infinity or at least at large distances from the origins of the generating or scattering mechanism. This unbounded domain generally poses a difficulty in the conventional finite element or finite difference analysis of the problem: it requires an unacceptably large computational domain; moreover, the accuracy of the numerical solution is not warranted because the solution is often affected by the location of the open boundaries where the domain is artificially truncated for computational convenience.

In finite element analysis, despite the success of using the hybrid element method (HEM)[1–6] and the infinite element method (IEM)[7–12] in dealing with this unbounded domain problem, both methods are complex in the programming and computation, which in turn may limit the methods only to certain applications. HEM requires that an analytic solution, which allows unknown coefficients, be obtained in the far region and a functional based on the first variational principle be constructed in the near region. In addition, the method tends to destroy the sparsity of the matrices used in the conventional finite element method and increases the programming and computational burden. On the other hand, while IEM preserves the same programming effort and computational efficiency as that of the conventional finite element method, the use of

* OPC Contribution No. 27.

Received April 1989
Revised June 1989

correct shape and mapping functions and simple numerical integration remains to be explored further.

In this paper a one- and a two-dimensional boundary value problem for water wave radiation and scattering in an unbounded water domain are formulated. The governing equations are Webster's horn equation for the one-dimensional problem and Berkhoff's equation for the two-dimensional problem. IEM is employed for solutions. The functionals, based on the first variational principle, are presented. In IEM we use conventional finite elements in the near region and a new type of infinite elements in the far region to approximate the solution. Two kinds of infinite elements, which exactly satisfy the one-dimensional and two-dimensional Sommerfeld radiation condition respectively, are presented. The attractive features of these infinite elements are: the shape and mapping functions are simple; all the integrals involving the infinite elements can be integrated analytically; and no numerical integration is required. These features result in simple programming and efficient computation. Applications are initially shown for the one-dimensional boundary value problem, followed by the two-dimensional boundary value problem.

FORMULATION AND CALCULATION

In linear wave theory, if a wave varies with time as $e^{-i\omega t}$, the wave motion can be characterized by the function $\phi(\mathbf{x})e^{-i\omega t}$, where ϕ is the velocity potential, which is a complex function of $\mathbf{x}$, $\mathbf{x}$ represents the spatial co-ordinates and t denotes time. Also, $i=\sqrt{(-1)}$, ω is the wave radian frequency, k is the wave number, $h(\mathbf{x})$ is the water depth and g is the gravitational acceleration. Then the dispersion relation is $\omega^2=gk\tanh kh$, the phase velocity is $c=\omega/k$ and the group velocity is $c_g=\partial\omega/\partial k$.

One-dimensional boundary value problem

The velocity potential in a channel of variable width b is given as a solution of

$$\frac{\mathrm{d}}{\mathrm{d}x}\lambda bcc_g\frac{\mathrm{d}\phi}{\mathrm{d}x}+bcc_gk^2\phi=0. \tag{1}$$

Here λ is the friction factor,[5]

$$\lambda=\left(1+\frac{i\beta a_0}{h\sinh kh}e^{i\gamma}\right)^{-1}, \tag{2}$$

where β is the friction coefficient, γ is the phase difference and a_0 is the incident wave amplitude. Equation (1) can be readily obtained by laterally integrating Berkhoff's equation (17) given later in the two-dimensional problem. In general, λ is a complex function; its imaginary part causes wave damping and is a small positive value in most cases. If there is no friction, i.e. $\lambda=1$, then (1) reduces to Webster's horn equation. Without loss of generality we consider a channel consisting of a straight channel of constant width b_0 and a channel of fan shape as shown in Figure 1(a). The governing equation is Webster's horn equation with $h=$constant (hence c and c_g are constants):

$$\frac{\mathrm{d}}{\mathrm{d}x}b\frac{\mathrm{d}\phi}{\mathrm{d}x}+bk^2\phi=0. \tag{3}$$

The boundary condition at the left-hand end of the channel is specified as a wave generator such that

$$\frac{\mathrm{d}\phi}{\mathrm{d}x}=\frac{gka_0}{\omega},\quad x=0. \tag{4}$$

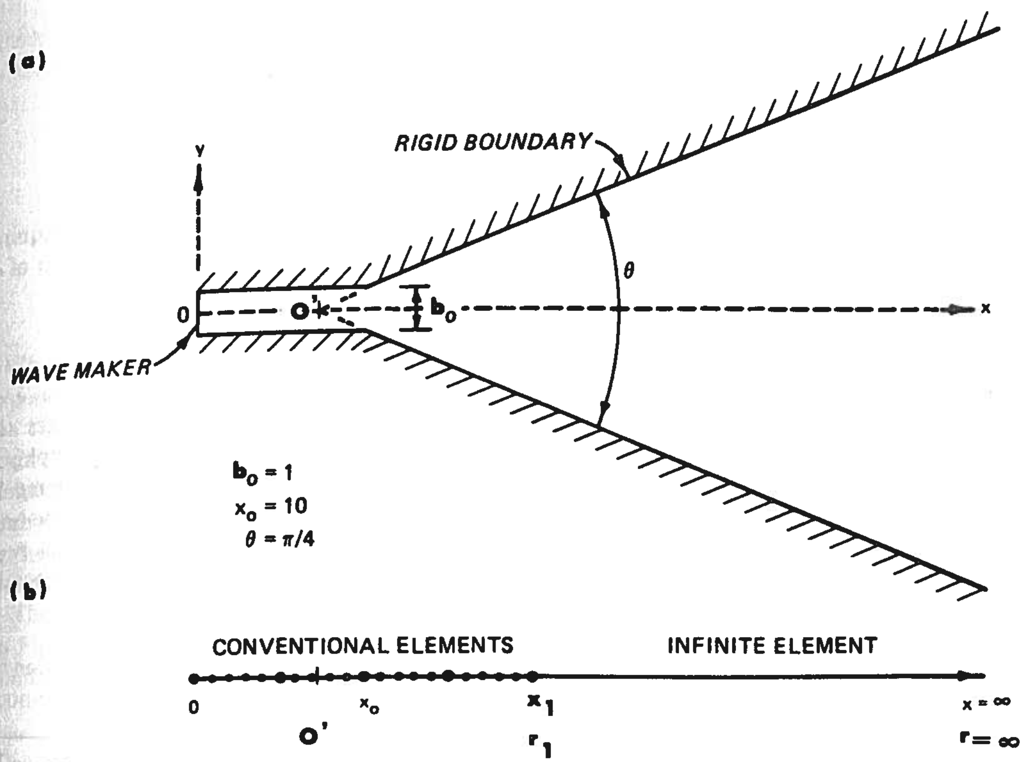

Figure 1. (a) Definition sketch and (b) network of finite and infinite elements of a one-dimensional channel

The Sommerfeld radiation condition is imposed at the right-hand end (at infinity) of the channel:

$$\lim_{x\to\infty}\sqrt{x}\left(\frac{\mathrm{d}}{\mathrm{d}x}-ik\right)\phi=0. \tag{5}$$

This condition requires $\phi\sim x^{-1/2}\,e^{ikx}$ at $x\to\infty$.

The analytical solution of the boundary value problem can be obtained to be

$$\frac{\phi}{ia_0}=\begin{cases}\dfrac{\cos k(x-x_0)H_0(kr_0)+\sin k(x-x_0)H'_0(kr_0)}{\cos kx_0H'_0(kr_0)+\sin kx_0H_0(kr_0)} & \text{if } 0\leqslant x\leqslant x_0,\\[2ex] \dfrac{H_0(kr)}{\cos kx_0H'_0(kr_0)+\sin kx_0H_0(kr_0)} & \text{if } x_0\leqslant x,\end{cases} \tag{6}$$

where $H_n(\cdot)$ and $H'_n(\cdot)$ are Hankel functions of the first kind and their derivatives respectively, x_0 is the length of the straight channel, θ is the angle of the fan channel, $r_0=b_0/\theta$ and

$$r=\frac{b_0}{\theta}+x-x_0. \tag{7}$$

Also,

$$b=\begin{cases} b_0, & 0\leqslant x\leqslant x_0, \\ r\theta, & x_0\leqslant x\leqslant\infty. \end{cases} \tag{8}$$

Later, equation (6) is used for comparison with the infinite element solution.

Infinite element solution. The variational principle for the boundary value problem requires that the following functional, Π_1, be stationary with respect to an arbitrary first variation of ϕ. The functional is given as

$$\Pi_1(\phi)=-\frac{1}{2}\int_0^\infty b\left(\frac{\mathrm{d}\phi}{\mathrm{d}x}\right)^2 \mathrm{d}x+\frac{1}{2}\int_0^\infty bk^2\phi^2\,\mathrm{d}x-\left[\frac{gka_0}{\omega}b\phi\right]_{x=0}+\tfrac{1}{2}\left[ikb\phi^2\right]_{x=\infty}. \tag{9}$$

The integrals in (9) involve integration over an infinite line domain, which makes the conventional finite element discretization and solution invalid. In this example IEM is employed to obtain the solution; we use the two-node linear elements in the near region, i.e. in the region from the wave generator to some distance beyond the end of the straight channel, and one one-node infinite element in the far region (Figure 1(b)). Since the two-node linear element has been extensively described by Zienkiewicz[13] and others, only the one-node infinite element is subsequently described.

Infinite element. Inspired by the asymptotic requirement of the solution at $x\to\infty$, equation (5) (also the asymptotic form of the Hankel function at $kr\to\infty$ for (6)), we construct the one-node infinite element specified by the following shape function:

$$N_{r1}=\sqrt{\left(\frac{r_1}{r}\right)}\exp[ik(r-r_1)],\quad 0<r_1\leqslant r\leqslant\infty, \tag{10}$$

where r is the local co-ordinate with the origin O' at the origin of the fan channel as shown in Figure 1(a); the relation between x and r is given by (7). In this case r_1 divides the near and the far region; the location of r_1 is chosen for computational convenience but can be at any location beyond the generating and scattering sources. The velocity potential of the infinite element is then approximated by

$$\phi=N_{r1}\phi_1, \tag{11}$$

where ϕ_1 is the nodal velocity potential to be solved. Also, $N_{r1}=1$ (hence $\phi=\phi_1$) at node $r=r_1$, which is a required nodal condition for the shape function; ϕ also exactly satisfies (5).

Discretization and calculation. Next, the entire domain is discretized into the two-node linear elements in the near region and one one-node infinite element in the far region as shown in Figure 1(b). The calculation of the element stiffness matrices for the two-node linear elements in the near region is no different than the conventional finite element method, which is not furnished here. The calculation of the element stiffness matrices for the one-node infinite element in the far region is carried out for the first two integrals of (9) from $x=x_1$ to ∞:

$$\begin{aligned}-\frac{1}{2}\int_{x_1}^\infty b\left(\frac{\mathrm{d}\phi}{\mathrm{d}x}\right)^2\mathrm{d}x&=-\frac{1}{2}\theta r_1\phi_1^2\int_{r_1}^\infty\left(-\frac{1}{2r}+ik\right)^2\exp[2ik(r-r_1)]\,\mathrm{d}r\\&=-\tfrac{1}{8}\{Y[1+\mathrm{e}^Y E_1(Y)]+1\}\theta\phi_1^2,\end{aligned} \tag{12}$$

$$\frac{1}{2}\int_{x_1}^\infty bk^2\phi^2\,\mathrm{d}x=\frac{1}{2}k^2 r_1\theta\phi_1^2\int_{r_1}^\infty\exp[2ik(r-r_1)]\,\mathrm{d}r=-\tfrac{1}{8}Y\theta\phi_1^2, \tag{13}$$

where $Y \equiv -2ikr_1$. In obtaining (12) and (13) we have invoked (7), (8), (10) and (11) and used the following exponential integral functions and their recurrence relations:[14]

$$E_n(z) = \int_1^{\infty} \frac{e^{-zt}}{t^n}\,dt \quad (n=0, 1, 2, 3, \ldots; \mathrm{Re}\, z \geqslant 0), \tag{14}$$

$$E_0(z) = -\frac{e^{-z}}{z}, \tag{15}$$

$$E_{n+1}(z) = \frac{1}{n}[e^{-z} - zE_n(z)] \quad (n=1, 2, 3, \ldots). \tag{16}$$

Clearly, all the integrals involving the infinite element are integrated analytically in terms of the exponential integral functions involving no numerical integration. The subroutine CEXPLI from the NSWC library[15] is used to calculate the exponential integral functions. Procedures to assemble the element matrices are straightforward, similar to those of the conventional finite element method. The numerical solution is then obtained by taking Π_1 stationary with respect to each nodal ϕ, followed by solving a set of the simultaneous linear equations. Note that the last term in (9) is immaterial because it vanishes as $x \to \infty$ owing to the existence of friction (if there is no friction, take $x \to \infty$ before letting $\lambda \to 1$) and thus is never calculated.

The numerical results of the absolute and real values of ϕ for $kx_0 = 1{\cdot}25\pi$ are shown in Figures (2a) and 2(b). The absolute difference between the numerical results and the exact solution (6) is less than 0·001.

Two-dimensional boundary value problem

The two-dimensional boundary value problem of water wave scattering by the presence of solid boundaries of arbitrary geometry and variable depth, as shown in Figure 3, has been formulated by Chen[5] and others. The governing equation is

$$\frac{\partial}{\partial x}\lambda cc_g \frac{\partial \phi}{\partial x} + \frac{\partial}{\partial y}\lambda cc_g \frac{\partial \phi}{\partial y} + cc_g k^2 \phi = 0. \tag{17}$$

Along the solid wall the following absorbent boundary condition is adopted:

$$\frac{\partial \phi}{\partial n} - \alpha\phi = 0, \qquad \alpha = ik\frac{1-K_r}{1+K_r}, \tag{18}$$

where n is the unit normal vector outward from the water domain and K_r is the reflection coefficient of the wall.

Now let ϕ_s be the velocity potential of the scattered wave, which must satisfy (17) and be an outgoing wave at infinity. It is the total wave ϕ less the incident wave ϕ_0, i.e.

$$\phi_s = \phi - \phi_0. \tag{19}$$

In the far region the Sommerfeld radiation condition is imposed at infinity to ensure a unique solution. We consider both the one- and two-dimensional Sommerfeld radiation condition[16] in this problem; the one-dimensional Sommerfeld radiation condition applies to a channel (canal or river) and the two-dimensional one to an open coast/offshore water. The one-dimensional Sommerfeld radiation condition is

$$\lim_{x' \to \infty}\left(\frac{d}{dx'} - i\frac{k}{\sqrt{\lambda}}\right)\phi_s = 0, \tag{20}$$

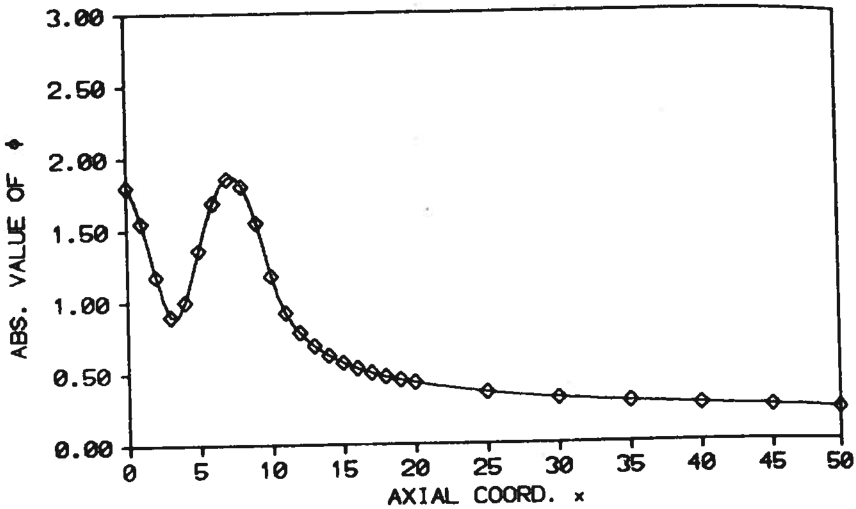

(a)

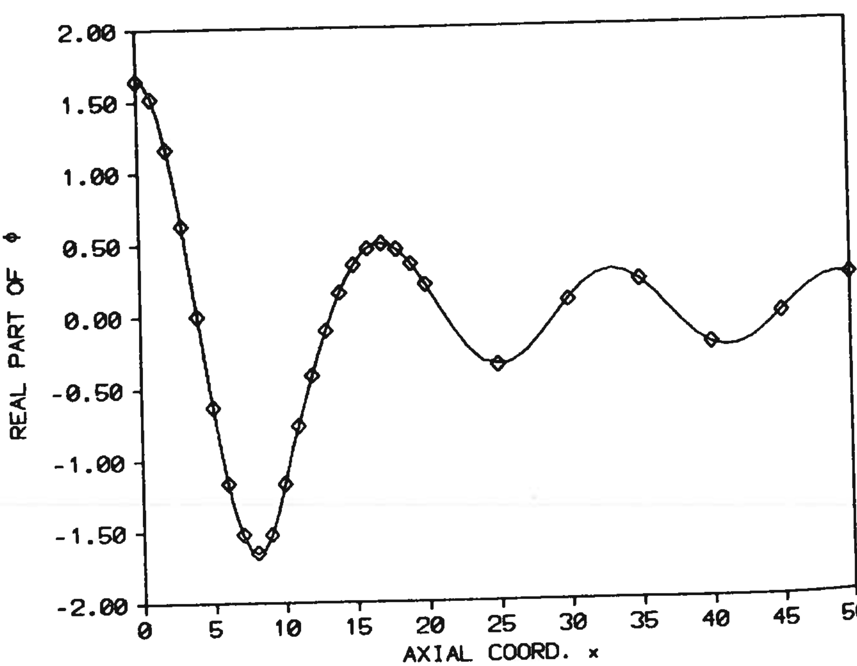

(b)

Figure 2. Comparison of (a) the absolute value of the velocity potential, $|\phi|$, and (b) the real part of the velocity potential $\mathrm{Re}\{\phi\}$ for $kx_0 = 1{\cdot}25\pi$: ——, analytical solution; ◇ ◇ ◇, IEM solution

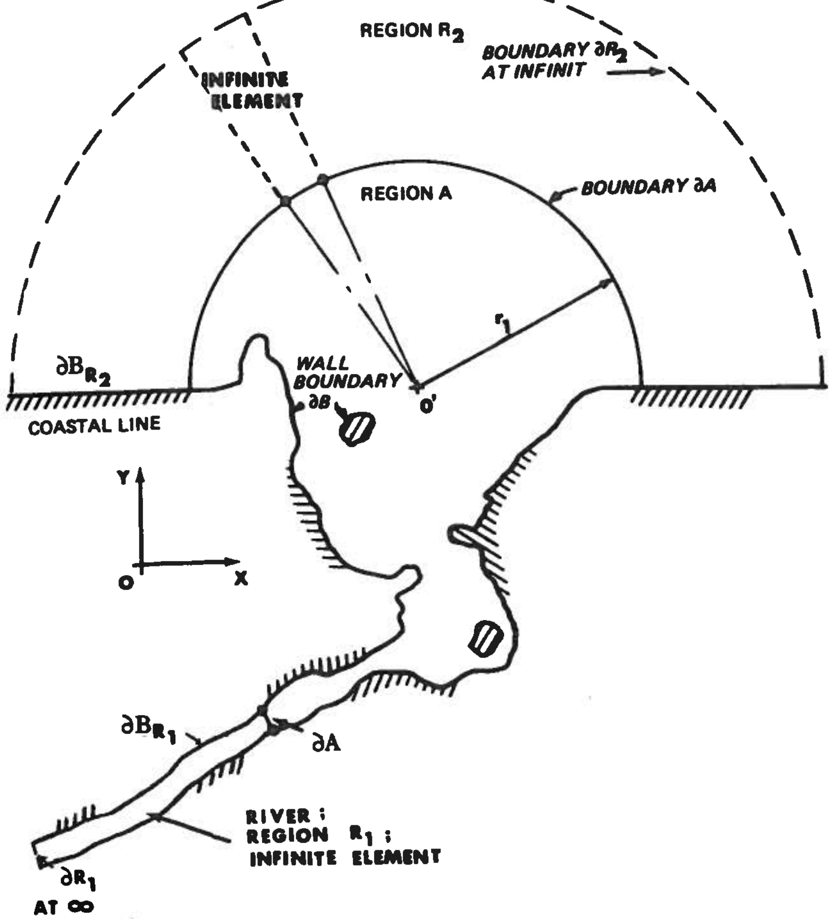

Figure 3. Definition sketch of the two-dimensional boundary value problem

where (x', y') are the local Cartesian co-ordinates as shown in Figure 4(a). This condition requires $\phi_s \sim \exp[i(k/\sqrt{\lambda})x']$ at $x' \to \infty$. The two-dimensional Sommerfeld radiation condition is

$$\lim_{r \to \infty} \sqrt{r}\left(\frac{\partial}{\partial r} - i\frac{k}{\sqrt{\lambda}}\right)\phi_s = 0, \tag{21}$$

where (r, θ) are the local polar co-ordinates as shown in Figure 4(b). This condition requires $\phi_s \sim (1/\sqrt{r})\exp[i(k/\sqrt{\lambda})r]$ at $r \to \infty$. Note that the expressions in parentheses for (20) and (21) are of the same form as (5) and are those usually used in most water wave problems, except for the friction factor λ.

Infinite element solution. Extension of IEM, used in the one-dimensional boundary value problem, to the two-dimensional boundary value problem presents no conceptual difficulties. The water domain is divided into three regions as illustrated in Figure 3: A is the near reion; R_1 is the far region of the one-dimensional Sommerfeld radiation condition; and R_2 is the far region of the

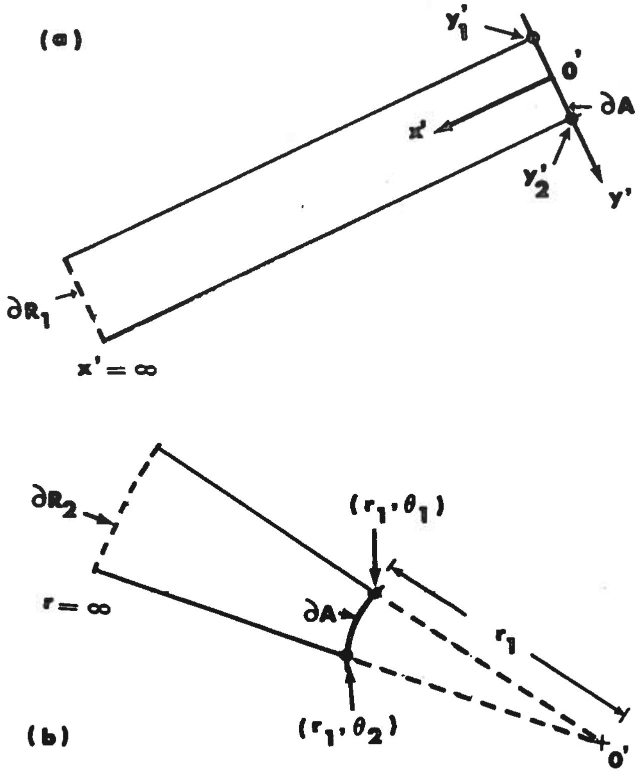

Figure 4. (a) Infinite element for the one-dimensional Sommerfeld radiation condition in R_1 and (b) infinite element for the two-dimensional Sommerfeld radiation condition in R_2

two-dimensional Sommerfeld radiation condition. In Figure 3 the lines ∂A separate A and $R_1 \cup R_2$ and their locations are chosen anywhere beyond the scattering origins; the lines ∂B are wall boundaries in the near region; the lines ∂B_{R_j} $(j=1, 2)$ are wall boundaries in the far regions R_j; and the lines ∂R_j are at infinity. The functional Π_2 for the boundary value problem using IEM for a solution is constructed as follows:

$$\begin{aligned}\Pi_2 = {} & \frac{1}{2}\iint_A [\lambda cc_g(\nabla\phi)^2 - cc_g k^2\phi^2]\,\mathrm{d}A - \frac{1}{2}\int_{\partial B} \alpha\lambda cc_g \phi^2\,\mathrm{d}L \\ & + \frac{1}{2}\iint_{R_1\cup R_2} [\lambda cc_g(\nabla\phi_s)^2 - cc_g k^2\phi_s^2]\,\mathrm{d}A - \int_{\partial A} \lambda cc_g \phi_s \frac{\partial\phi_0}{\partial n_A}\,\mathrm{d}L \\ & - \frac{1}{2}\int_{\partial B_{R_1}\cup\partial B_{R_2}} \alpha\lambda cc_g\phi_s^2\,\mathrm{d}L - \frac{1}{2}\int_{\partial R_1\cup\partial R_2} \mathrm{i}\frac{k}{\sqrt{\lambda}} cc_g\phi_s^2\,\mathrm{d}L,\end{aligned} \tag{22}$$

where $\mathrm{d}A$ and $\mathrm{d}L$ are the area and line differential operators respectively and n_A is the unit normal vector outwards from region A. Again, the integrals involving regions R_1 and R_2 are over an infinite domain, making direct application of the conventional finite element method invalid. In IEM we use three-node triangular linear elements in the near region and a new type of two-node infinite elements in the far region as approximations. The three-node linear element has also been extensively described;[13] thus only the two two-node infinite elements for R_1 and R_2 are described in the following section.

Infinite elements. In R_1 the infinite element of semi-infinite rectangular shape as shown in Figure 4(a) is used; the element domain is $0 \leqslant x' \leqslant \infty$ and $y'_1 \leqslant y' \leqslant y'_2$. On the basis the asymptotic behaviour of ϕ at $x' \to \infty$ we construct the two-node infinite element specified by the following shape functions:

$$N_{x'y'1} = \frac{y'_2 - y'}{y'_2 - y'_1} N_{x'}, \qquad N_{x'y'2} = \frac{y' - y'_1}{y'_2 - y'_1} N_{x'}, \tag{23}$$

where

$$N_{x'} = \exp\left(\mathrm{i}\frac{k}{\sqrt{\lambda}} x'\right), \quad 0 \leqslant x' \leqslant \infty, \tag{24}$$

and (x', y') are the local Cartesian co-ordinates as shown in Figure 4(a). The shape functions satisfy the nodal condition: $N_{x'y'1} = 1$ and $N_{x'y'2} = 0$ at $(0, y'_1)$; $N_{x'y'1} = 0$ and $N_{x'y'2} = 1$ at $(0, y'_2)$. The (scattered wave) velocity potential of the infinite element is written in terms of the two nodal velocity potentials ϕ_{s1} and ϕ_{s2} as follows:

$$\phi_s = N_{x'y'1}\phi_{s1} + N_{x'y'2}\phi_{s2}, \quad 0 \leqslant x' \leqslant \infty, \quad y'_1 \leqslant y' \leqslant y'_2. \tag{25}$$

Clearly ϕ_s of (25) exactly satisfies (20).

In R_2 the infinite element of the shape of a sector outside a circle as shown in Figure 4(b) is used; the element domain is $0 < r_1 \leqslant r \leqslant \infty$ and $\theta_1 \leqslant \theta \leqslant \theta_2$. The corresponding shape functions are

$$N_{r\theta 1} = \frac{\theta_2 - \theta}{\theta_2 - \theta_1} N_{r1}, \qquad N_{r\theta 2} = \frac{\theta - \theta_1}{\theta_2 - \theta_1} N_{r1}, \tag{26}$$

where

$$N_{r1} = \sqrt{\left(\frac{r_1}{r}\right)} \exp\left(\mathrm{i}\frac{k}{\sqrt{\lambda}}(r - r_1)\right), \quad 0 < r_1 \leqslant r \leqslant \infty, \tag{27}$$

and (r, θ) are the local polar co-ordinates; r_1 is the radius of ∂A as shown in Figure 4(b). The shape functions satisfy (21) as well as the nodal condition. The (scattered wave) velocity potential of the infinite element is written as follows:

$$\phi_s = N_{r\theta 1}\phi_{s1} + N_{r\theta 2}\phi_{s2}, \quad 0 < r_1 \leqslant r \leqslant \infty, \quad \theta_1 \leqslant \theta \leqslant \theta_2. \tag{28}$$

In the evaluation of Π_2, analogous to the one-dimensional boundary value problem, the calculation of the integrals over each element in the near region poses no difficulty; it is carried out using the same procedures of the conventional finite element method, procedures which we do not expound upon in this paper. In the far regions R_1 and R_2, by choosing (25) or (28) for each type of the infinite elements and invoking (14) through (16), the third, fourth and fifth integrals in (22) are integrated respectively as follows. In region R_2 the third integral becomes

$$\frac{1}{2}\int_{\theta_1}^{\theta_2}\int_{r_1}^{\infty} \lambda c c_g (\nabla\phi_s)^2 r \mathrm{d}r \mathrm{d}\theta = \frac{1}{2}\{\phi_s\}(\lambda c c_g)\begin{bmatrix} p & q \\ q & p \end{bmatrix}\{\phi_s\}^{\mathrm{T}}, \tag{29}$$

$$-\frac{1}{2}\int_{\theta_1}^{\theta_2}\int_{r_1}^{\infty} \frac{c_g \omega^2}{c}\phi_s^2 \, r \mathrm{d}r \mathrm{d}\theta = \frac{1}{2}\{\phi_s\}\frac{1}{24}(\lambda c c_g \Delta X)\begin{bmatrix} 2 & 1 \\ 1 & 2 \end{bmatrix}\{\phi_s\}^{\mathrm{T}}, \tag{30}$$

where $\{\phi_s\}$ is the array of the nodal (scattered wave) velocity potential of the infinite element and the superscript T is the transpose of the array, such that

$$\{\phi_s\} \equiv \{\phi_{s1}, \phi_{s2}\}, \qquad \{\phi_s\}^{\mathrm{T}} = \begin{Bmatrix} \phi_{s1} \\ \phi_{s2} \end{Bmatrix}. \tag{31}$$

Also,

$$p = \frac{\Delta}{12}\{1 + X[1 + \mathrm{e}^X E_1(X)]\} + \frac{1}{\Delta}[1 - X\,\mathrm{e}^X E_1(X)], \tag{32}$$

$$q = \frac{\Delta}{24}\{1 + X[1 + \mathrm{e}^X E_1(X)]\} - \frac{1}{\Delta}[1 - X\,\mathrm{e}^X E_1(X)] \tag{33}$$

and

$$\Delta = \theta_2 - \theta_1, \qquad X = -2\mathrm{i}\frac{k}{\sqrt{\lambda}} r_1. \tag{34}$$

The fourth and fifth integrals are

$$-\int_{\theta_1}^{\theta_2} \left(\lambda c c_g \frac{\partial \phi_0}{\partial r} \phi_s\right)_{r=r_1} r_1 \,\mathrm{d}\theta = \{\phi_s\}\left(-\lambda c c_g \frac{\partial \phi_0}{\partial r}\right)_{r=r_1} \frac{r_1 \Delta}{2} \begin{Bmatrix} 1 \\ 1 \end{Bmatrix}, \tag{35}$$

$$-\frac{1}{2}\int_{r_1}^{\infty} (\alpha \lambda c c_g \phi_s^2)_{\theta \text{ on } \partial \mathrm{B}_{\mathrm{R}_2}} \,\mathrm{d}r = \tfrac{1}{2}[-\alpha \lambda c c_g r_1 \,\mathrm{e}^X E_1(X) \phi_s^2]_{\theta \text{ on } \partial \mathrm{B}_{\mathrm{R}_2}}. \tag{36}$$

In region R_1 the integrations for the third, fourth and fifth integrals are

$$\frac{1}{2}\int_{y_1'}^{y_2'}\int_0^{\infty} \lambda c c_g (\nabla \phi_s)^2 \,\mathrm{d}x' \,\mathrm{d}y' = \frac{1}{2}\{\phi_s\}(\lambda c c_g)\begin{bmatrix} p' & q' \\ q' & p' \end{bmatrix}\{\phi_s\}^{\mathrm{T}}, \tag{37}$$

$$-\frac{1}{2}\int_{y_1'}^{y_2'}\int_0^{\infty} \frac{c_g \omega^2}{c} \phi_s^2 \,\mathrm{d}x' \,\mathrm{d}y' = \frac{1}{2}\{\phi_s\}\frac{1}{24}(\lambda c c_g X')\begin{bmatrix} 2 & 1 \\ 1 & 2 \end{bmatrix}\{\phi_s\}^{\mathrm{T}}, \tag{38}$$

$$-\int_{y_1'}^{y_2'} \left(\lambda c c_g \frac{\partial \phi_0}{\partial x'} \phi_s\right)_{x'=0} \mathrm{d}y' = \{\phi_s\}\left(-\lambda c c_g \frac{\partial \phi_0}{\partial x'}\right)_{x'=0} \frac{\Delta'}{2}\begin{Bmatrix} 1 \\ 1 \end{Bmatrix}, \tag{39}$$

$$-\frac{1}{2}\int_0^{\infty} (\alpha \lambda c c_g \phi_s^2)_{y' \text{ on } \partial \mathrm{B}_{\mathrm{R}_1}} \,\mathrm{d}x' = \frac{1}{2}\left(\frac{-\alpha \lambda c c_g \Delta'}{X'} \phi_s^2\right)_{y' \text{ on } \partial \mathrm{B}_{\mathrm{R}_1}}, \tag{40}$$

where we define

$$p' = \frac{X'}{12} + \frac{1}{X'}, \qquad q' = \frac{X'}{24} - \frac{1}{X'} \tag{41}$$

and

$$\Delta' = y_2' - y_1', \qquad X' = -2\mathrm{i}\frac{k}{\sqrt{\lambda}}\Delta'. \tag{42}$$

Therefore all integrals for each infinite element now are integrated analytically with results given in terms of the exponential integral function $E_1(\cdot)$; again, no numerical integration is

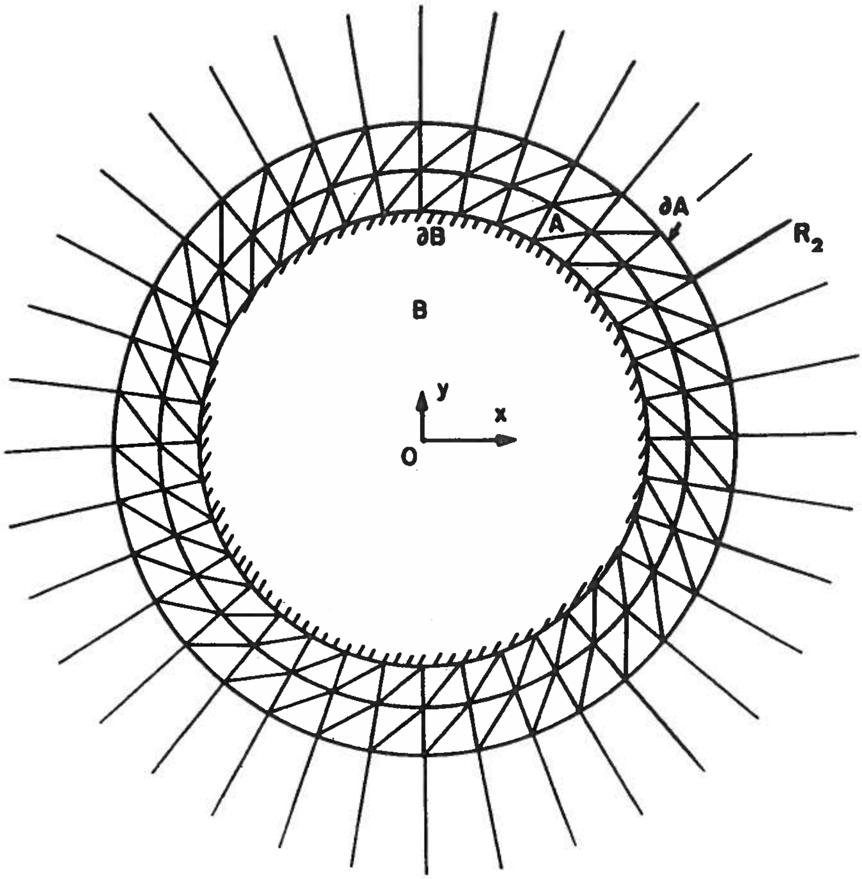

Figure 5. Network of finite and infinite elements for a circular cylinder

required. The last integral of Π_2 is immaterial for the same reason given in the one-dimensional boundary value problem. In performing the variational procedures to obtain the solution, we have used (19) and $\delta\phi_s = \delta\phi$ on ∂A (δ is the variational operator), i.e. $\delta\phi_0 = 0$ since the incident wave is a given function. Now, for a given incident wave ϕ_0 and $\partial\phi_0/\partial n$ on ∂A, an efficient solution is then obtained through the same procedure as that of the conventional finite element method.

Examples. Numerical results are shown for two cases: one for a vertical circular cylinder and the other for a rectangular harbour. For the former case the network of finite and infinite elements is shown in Figure 5. In the calculation a plane incident wave train is given as

$$\phi_0 = -\frac{iga_0}{\omega} \exp[ikr\cos(\theta - \theta_0)], \tag{43}$$

where θ_0 is the incident wave angle. We also assume that there is no friction ($\lambda = 1$) and a perfectly reflecting wall ($K_r = 1$). The absolute difference between the numerical results and the analytical solution is less than 0·03 as indicated in Figure 6. For the latter case the network of finite and

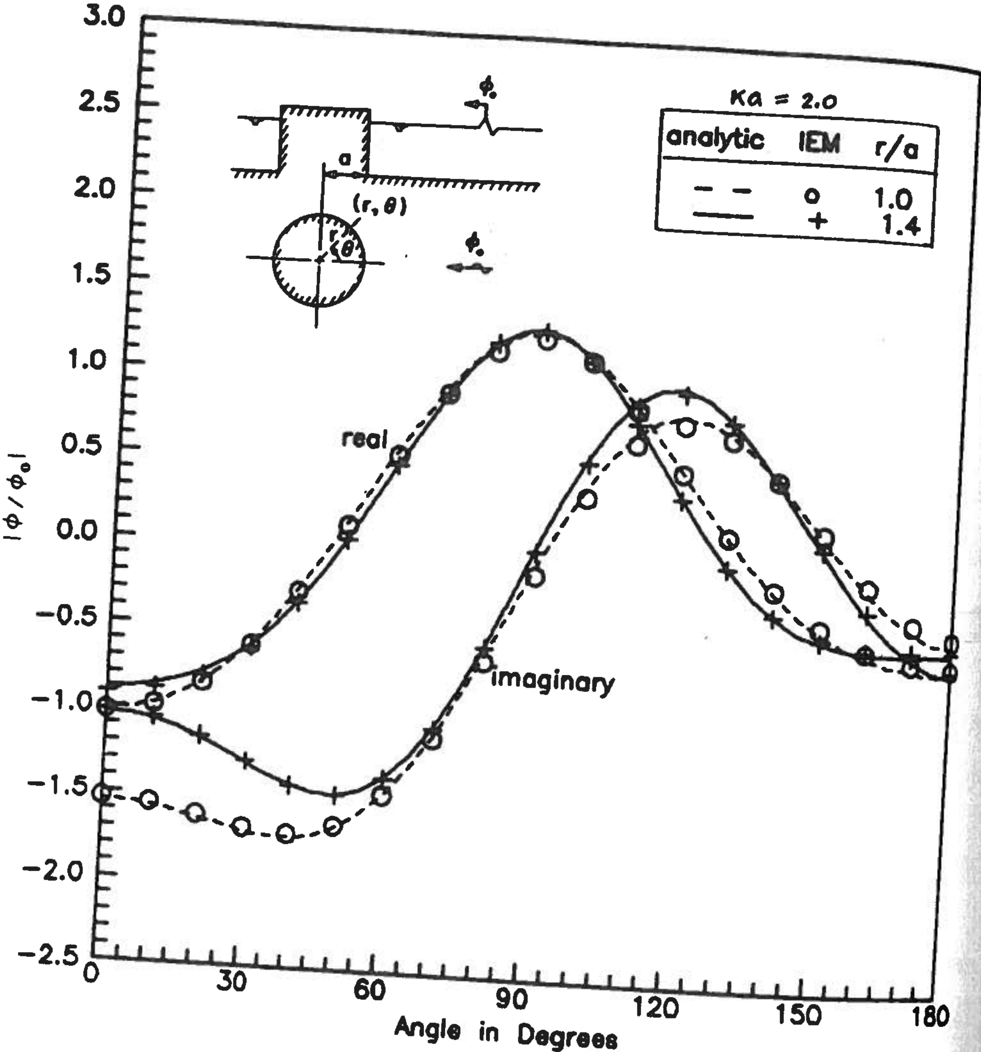

Figure 6. Comparison of analytical and IEM results for a circular cylinder

infinite elements is shown in Figure 7. We assume that an exciting wave train is the sum of an incident and a reflected wave on a partially reflecting wall:

$$\phi_0 = -\frac{iga_0}{\omega}\{\exp[ikr\cos(\theta-\theta_0)] + K_r \exp[ikr\cos(\theta-\theta_0)]\}, \tag{44}$$

where the wave field is specified with and without the effect of the bottom friction. For the case without friction and with perfect reflection, agreement between the numerical results and the analytical solutions and other numerical results[1,4] is to two decimal places as indicated in Figure 8. For the case with friction and an absorbent wall (there is no analytical solution available for this case) the numerical results agree fairly well with laboratory data and other numerical

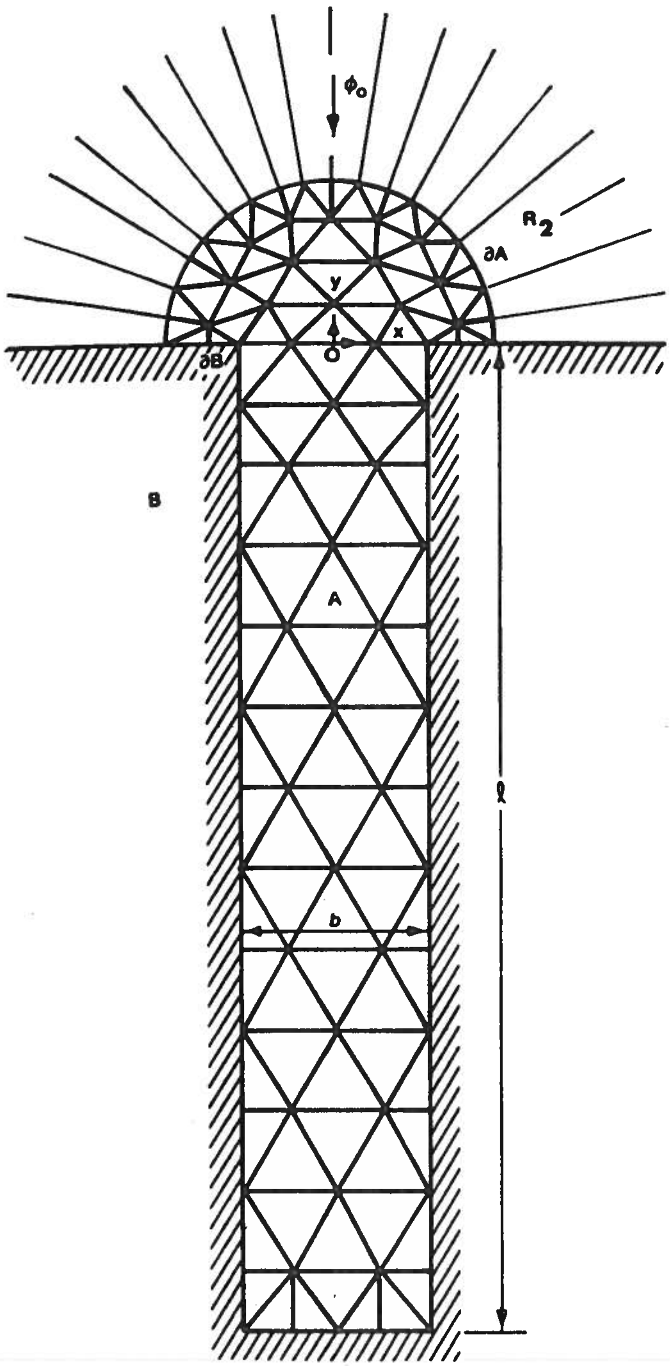

Figure 7. Network of finite and infinite elements for a rectangular harbour; $b=6{\cdot}04$ cm, $l=31{\cdot}11$ cm, water depth $h=25{\cdot}72$ cm

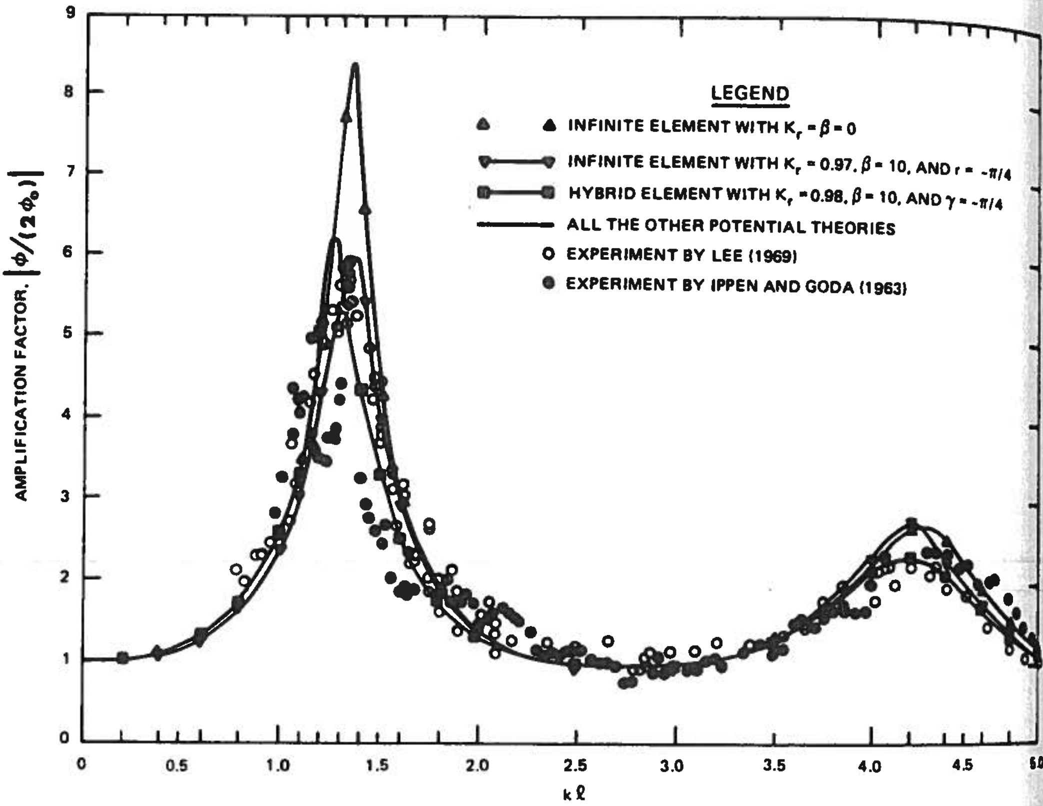

Figure 8. Comparison of the amplification factor $|\phi|/2a_0$ at the centre of the back wall of the harbour

results,[1,4] except near the resonance peaks where the difference in peak value and phase is discernible, as also indicated in Figure 8.

CONCLUSIONS

The mathematical formulations of the one- and two-dimensional boundary value problems for water wave radiation and scattering in an unbounded domain are presented, along with their functionals. The functionals are constructed assuming that IEM is used to obtain a solution. The two new infinite elements are constructed on the basis of the asymptotic behaviour of the scattered waves at infinity. The shape functions are simple and satisfy the nodal condition as well as the Sommerfeld radiation condition. The integrals of the functionals for the infinite elements are integrated analytically without the need to employ numerical integration. The programming and computational efforts are similar to those of the conventional finite element method. For the test cases presented the numerical results are acceptably accurate when compared with the data and exact solutions.

REFERENCES

1. H. S. Chen and C. C. Mei, 'Oscillations and wave forces in an offshore harbor', *Ralph M. Parsons Lab., Report 190*, MIT, August 1974.

2. D. K. P. Yue, H. S. Chen and C. C. Mei, 'A hybrid element method for diffraction of water waves by three-dimensional bodies', *Int. j. numer. methods eng.*, **12**, 245–266 (1978).
3. H. S. Chen, 'Calculation of water wave scattering with friction', *EMD Specialty Conf.*, ASCE, August 1984, pp. 716–719.
4. H. S. Chen, 'Hybrid element modeling of harbor resonance', *4th Int. Conf. on Applied Numerical Modeling*, December 1984, pp. 312–316.
5. H. S. Chen, 'Effects of bottom friction and boundary absorption on water wave scattering', *Appl. Ocean Res.* **8**, 99–104 (1986).
6. H. S. Chen and J. R. Houston, 'Calculation of water oscillation in coastal harbors: HARBS and HARBD user's manual', *IR CERC-87-2*, U.S. Army Engineer Waterways Experiment Station, April 1987.
7. P. Bettess, 'Infinite elements', *Int. j. numer. methods eng.*, **11**, 53–64 (1977).
8. P. Bettess and O. C. Zienkiewicz, 'Diffraction and refraction of surface waves using finite and infinite elements', *Int. j. numer. methods eng.*, **11**, 1271–1290 (1977).
9. P. Bettess, 'More on infinite elements', *Int. j. numer. methods eng.*, **15**, 1613–1626 (1980).
10. O. C. Zienkiewicz, C. Emson and P. Bettess, 'A novel boundary infinite element', *Int. j. numer. methods eng.*, **19**, 393–404 (1983).
11. J. D. Pos, 'Asymmetrical breakwater gap wave diffraction using finite and infinite elements', *Coastal Eng.*, **9**, 101–123 (1985).
12. O. C. Zienkiewicz, K. Bando, P. Bettess, C. Emson and T. C. Chiam, 'Mapped infinite elements for exterior wave problems', *Int. j. numer. methods eng.*, **21**, 1229–1251 (1985).
13. O. C. Zienkiewicz, *The Finite Element Method in Engineering Science*, McGraw-Hill, 1971.
14. M. Abramowitz and I. A. Stegun, *Handbook of Mathematical Functions with Formulas, Graphs, and Mathematical Tables, NBS Appl. Math. Ser. 55*, June 1964, pp. 228–230.
15. A. H. Morris Jr, 'NSWC library of mathematics subroutines', Naval Surface Weapons Center, June 1984, pp. 27–29.
16. A. Sommerfeld, *Partial Differential Equations in Physics, Lectures on Theoretical Physics, Vol. VI*, Academic Press 1964, pp. 188–200.